RAPID COMMUNICATIONS

PHYSICAL REVIEW A VOLUME 46, NUMBER 2 15 JULY 1992

Geometrical anchoring at an inclined surface of a liquid crystal

O. D. Lavrentovich*

Laboratoire de Physique des Solides, Université de Paris-Sud, Bât. 510, 91405 Orsay CEDEX, France and Institute of Physics, Academy of Sciences of the Ukraine, pr. Nauki, 46, Kyïv, Ukraine

(Received 8 April 1992)

The free energy of a nematic film, placed between two isotropic media, does not depend on the azimuthal angle if the two interfaces are parallel. It is shown that in the general case of nonparallel bounding, a particular value of the azimuthal orientation is energetically preferable. The directions of this geometrically imposed easy axis and of the thickness gradient need not necessarily coincide. The geometrical anchoring may induce the twist deformations and force the nematic liquid crystal to behave like an optically active object.

PACS number(s): 61.30.Gd, 68.10.Cr, 68.10.Gw

Molecular interactions at the interface between a liquid crystal and an ambient medium establish a definite orientation of the director **n**, which is described by the polar angle $\bar{\theta}$ and the azimuthal angle $\bar{\phi}$; $(\bar{\theta},\bar{\varphi})$ is called the easy axis. If the liquid crystal is in contact with an isotropic medium (isotropic liquid, gas, special rigid plate) the surface free energy is azimuthally independent and only $\bar{\theta}$ is fixed [1–5]. Thus the azimuthal reorientations of the nematic film, placed between two isotropic media, do not change the energy of the system. Simple examples considered in this Rapid Communication show that this statement is valid only in a particular case when the liquid crystal is placed between two parallel flat plates. In the general case of nontrivial bounding the surface tilt leads to well-defined azimuthal orientation which corresponds to the minimum of the free elastic energy. The directions of this geometrically imposed easy axis and of the thickness gradient need not necessarily coincide. Moreover, the geometrical anchoring may induce the twist deformations, and force the nematic sample to behave like an optically active object in spite of the nonactivity of the nematic liquid crystal and the ambient media themselves.

Let us call Z the normal to the lower plate of the cell, θ the polar angle between **n** and Z, and φ the angle in the (X,Y) plane. We consider the configurations

$$(n_x;n_y;n_z)=(\sin\theta(z)\cos\phi(z);\sin\theta(z)\sin\phi(z);\cos\theta(z)) \tag{1}$$

for two nematic cells with the same strong tangential orientation at the upper boundary but generally different anchoring at the lower one (Fig. 1): In the A cell the easy axes are distributed on a cone,

$$\theta(z=0)=\bar{\theta}=\text{const},\quad 0\le\bar{\theta}\le\pi/2\,, \tag{2}$$

while in the B cell there is a unidirectional tangential anchoring,

$$\theta(z=0)=\pi/2,\quad \varphi(z=0)=0\,. \tag{3}$$

Thus the A cell can represent the nematic film bounded by two isotropic media; the B cell corresponds, for example, to the nematic film placed on the rigid support with unidirectional treatment. In both cells the orientation at the upper surface is tangential and azimuthally degenerated, $\theta(z=d)=\pi/2$. Let us assume that this surface is inclined around the Y axis (Fig. 1). Now, $\theta(z=d)$ depends on the inclination angle γ and on the azimuthal parameter φ_0, which is the angle between **n** and a fixed axis X' in the inclined plane:

$$\theta(z=d)=\arccos(\sin\gamma\cos\varphi_0)\,. \tag{4}$$

In the A case the twist deformations can be eliminated from the consideration due to the azimuthal degeneracy of the boundary conditions, and the free-energy density is

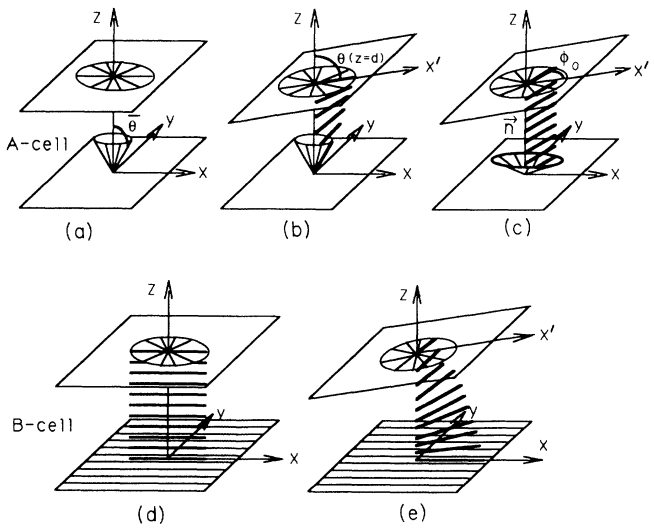

FIG. 1. The geometry of anchoring and tilting of the A cell [(a)–(c)] and the B cell [(d),(e)]. The A cell can be aligned initially uniformly (the difference in polar anchoring $\Delta\bar{\theta}=0$) or in a hybrid manner ($\Delta\bar{\theta}\neq 0$) (a). The surface tilt leads to the preferable orientation of the director **n** along $\varphi_{0eq}=0$, if $0<\gamma\le\Delta\bar{\theta}$ (b), or along nonzero φ_{0eq}, if $\gamma>\Delta\bar{\theta}$ (c). The B cell is initially aligned tangentially ($\Delta\bar{\theta}=0$); this orientation is unidirectional at the lower plate and degenerated at the upper one (d). The balance between the geometrical anchoring induced by the tilt and the physical anchoring induced by the unidirectional rubbing, results in the twist of **n** (e).

$$f=\tfrac{1}{2}K\theta_z^2, \tag{5}$$

where the splay (K_{11}) and bend (K_{33}) elastic constants are taken to be equal, $K_{11}=K_{33}=K$; the subscript z means the derivative with respect to z. The variational calculation of the state of minimum free energy provides a bulk equation:

$$\theta_{zz}=0. \tag{6}$$

The solution satisfying the boundary conditions (2) and (4),

$$\theta(z)=\bar{\theta}+[\arccos(\sin\gamma\cos\varphi_0)-\bar{\theta}]z/d, \tag{7}$$

leads to the φ_0-dependent free energy calculated per unit area at the horizontal plane [Fig. 2(a)],

$$F_A=F_0+W_g$$
$$=\frac{K}{2d}(\Delta\bar{\theta})^2+\frac{K}{2d}\{[\arcsin(\sin\gamma\cos\varphi_0)]^2 - 2\Delta\bar{\theta}\arcsin(\sin\gamma\cos\varphi_0)\}; \tag{8}$$

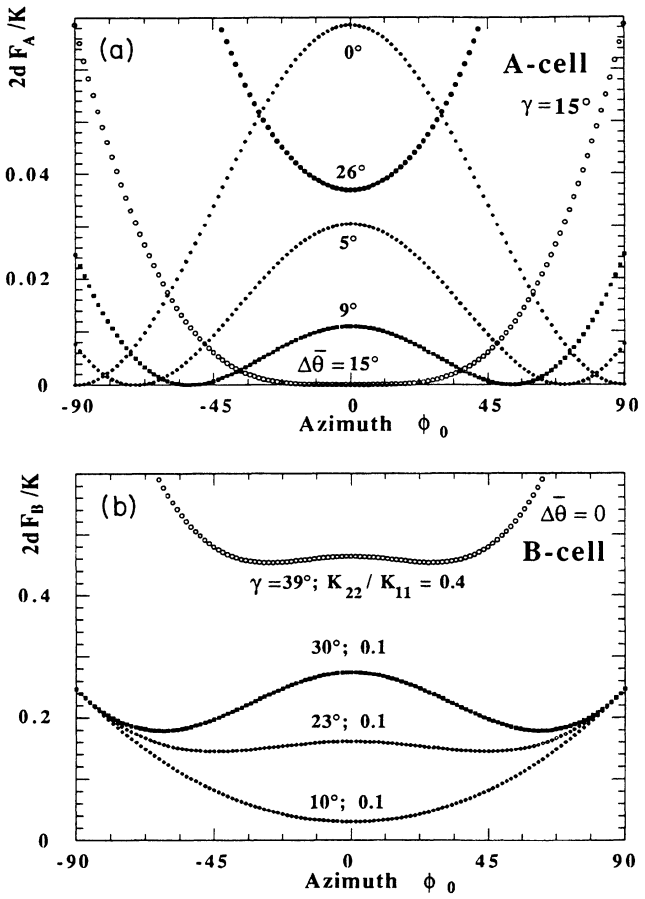

FIG. 2. The dependences of the elastic energies on the azimuthal parameter φ_0 for (a) the A cell and (b) the B cell, calculated from Eqs. (8) and (12), respectively. For the A cell the tilt angle is taken as constant ($\gamma=15°$); different $\Delta\bar{\theta}$ lead to different preferable azimuthal orientations. For the B cell the twist deformations increase with the increase of γ and with the decrease of K_{22}/K_{11}.

here d is the local thickness of the cell and $\Delta\bar{\theta}=\pi/2-\bar{\theta}$ is the difference in the polar anchoring at two surfaces. The second term of Eq. (8) can be considered as the geometrical anchoring function W_g with well-defined angular dependency.

The minimization of F_A with respect to φ_0 shows that the surface tilt imposes a preferred azimuthal orientation. If $0<\gamma\leq\Delta\bar{\theta}$, the easy axis is aligned along the thickness gradient, $\varphi_{0eq}=0$ [Figs. 1(b) and 2(a)]. With constant γ the increase of $\Delta\bar{\theta}$ leads to more sharp minimum in $F_A(\varphi_0)$. In the opposite case, $\gamma>\Delta\bar{\theta}$, one finds nonzero solutions [Figs. 1(c) and 2(a)]:

$$\varphi_{0eq}=\pm\arccos(\sin\Delta\bar{\theta}/\sin\gamma). \tag{9}$$

Any deviation from these "geometrical" easy axes will lead to the increase of the free energy, Fig. 2(a). These results are clear to understand. For example, if the lower plate sets the tangential orientation, $\Delta\bar{\theta}=0$, the nematic is absolutely uniform only for $\varphi_{0eq}=\pm\pi/2$, and any other φ_0 implies the splay distortions.

Now let us imagine that one of the plates imposes "physical" azimuthal anchoring [$\varphi(z=0)=0$, for example]. The optimum state will be achieved by a balance between the splay and twist deformations, Figs. 1(d) and 1(e). This is the case of the B cell. The experimental data [6–9] for the corresponding geometry display an optical activity of the nematic drops placed at the rubbed or polished rigid plate. The origin of this distracted phenomena is still debated [9]. The geometrical anchoring provides quite a natural explanation.

In equilibrium the untilted B cell displays $\theta(z)=\pi/2$ and $\varphi(z)=0$. When the upper boundary is slightly inclined, one has a deviation from this state, $\theta(z)\rightarrow\pi/2+\theta_1(z)$ and $\varphi(z)\rightarrow 0+\varphi_1(z)$. To the second order in θ_1, the free-energy density is defined by the splay and twist terms with corresponding elastic constants K_{11} and K_{22}:

$$f=\tfrac{1}{2}K_{11}\theta_{1z}^2+\tfrac{1}{2}K_{22}\varphi_{1z}^2. \tag{10}$$

The bulk equations

$$\theta_{1zz}=0,\ \varphi_{1zz}=0, \tag{11}$$

with the conditions (3) and (4), lead to the free energy per unit area:

$$F_B=\frac{K_{11}}{2d}[\arcsin(\sin\gamma\cos\varphi_0)]^2 + \frac{K_{22}}{2d}\left[\arctan\left(\frac{\tan\varphi_0}{\cos\gamma}\right)\right]^2. \tag{12}$$

The last expression shows that the equilibrium azimuthal angle at the upper boundary can be nonzero, Fig. 2(b). It implies the presence of twist deformations and hence the optical activity of the sample. The latter was detected by Meyerhofer, Sussman, and Williams [8] for a sessile nematic drop which must possess a curved upper surface except in the rare case of complete wetting. Especially pronounced twist effect due to the geometrical anchoring is expected for the nematic liquid crystal poly-γ-benzyl-glutamate, where the ratio K_{22}/K_{11} can be as small

as 0.1 and even less [10]. For the exact quantitative description of the sessile drop or similar problem, one should take into account also the three-dimensional nature of the problem, the finite values of physical anchoring as well as of elastic constants K_{24} and K_{13}. However, these factors do not change the main conclusion that consists in prediction of preferred azimuthal orientation and twist deformations due to the nonflat bounding.

One should distinguish the geometrical anchoring from the coupling between the shape of the nematic-isotropic interface and the elastic distortions of the nematic bulk, which was considered by de Gennes [1,11]. As discussed in [1,11], the elastic energy of the nonuniform nematic liquid crystal can be reduced by the interface tilt if the interfacial tension and the density difference of the two media are sufficiently small. On the contrary, the geometrical anchoring does not imply the discussed balance; the bulk distortions can be negligibly small and the interfacial tension can be infinitely large. All that is needed is just the geometrical tilt of the surface, which can be induced by any external factor, including the interface tension. In this respect the situation is closer to the Berreman's anchoring at the rubbed surface [12] and may lead to important consequences for the technology of preparation of the nematic cells, especially when the oblique evaporation of the orientants is used.

The geometrical-anchoring approach can be applied to different geometries and media. For example, the smectic A phase in the A geometry with $\bar{\theta}=\pi/2$ should reorient $\mathbf{n}$ along the (Z,Y) plane to avoid the splay deformations caused by the tilt. Interesting behavior is expected for the spreaded liquid-crystalline films in wetting or partial wetting regimes, which are practically unstudied. One example is illustrated (Fig. 3) and described below for the micrometer-thick nematic film, placed between two isotropic media that impose different polar orientation of $\mathbf{n}$.

A small drop (5–10 mg) of the nematic liquid crystal penthylcyanobiphenyl (5CB) has been spreaded onto the glycerine substrate, which gives rise to the tangential orientation of $\mathbf{n}$ at the lower film boundary [13]. The upper film surface has been left free; the free surface of 5CB provides the normal orientation [5]. After a few hours the spreading stops, due to the finite surface area of the container (60 cm^2) and the possible role of long-range cohesive forces [14]. Typical spreading area was 20–50 cm^2.

The resulting film structure is determined by the film profile, nematic elasticity, polar physical and azimuthal geometrical anchoring, as well as by shear during the spreading. In order to remove the possible influence of the shear the sample has been heated to 60 °C, which is ≈ 25 °C above the nematic to isotropic phase transition temperature for 5CB, and then cooled again to the nematic phase. It turned out that the essential features of the film structure that are described below do not depend on the number of the thermal cycles and thus are not related to the shear deformations. Nevertheless, the textures are drastically different along the film radius. As it follows from the polarizing-microscopy observations with quartz wedge, there are three different regions (Fig. 3).

(1) The thin "precursor" part where the horizontal projection $\mathbf{n}_{xy}$ of $\mathbf{n}$ is oriented along the thickness gradient, $\varphi_0=0$. This alignment appears after each thermal cycle and is quite uniform throughout the film periphery, except narrow band in the thinnest part of the precursor which is occupied by stripe domains [15] with small deviations from $\varphi_0=0$. They are invisible in the Fig. 3(a) because of small magnification.

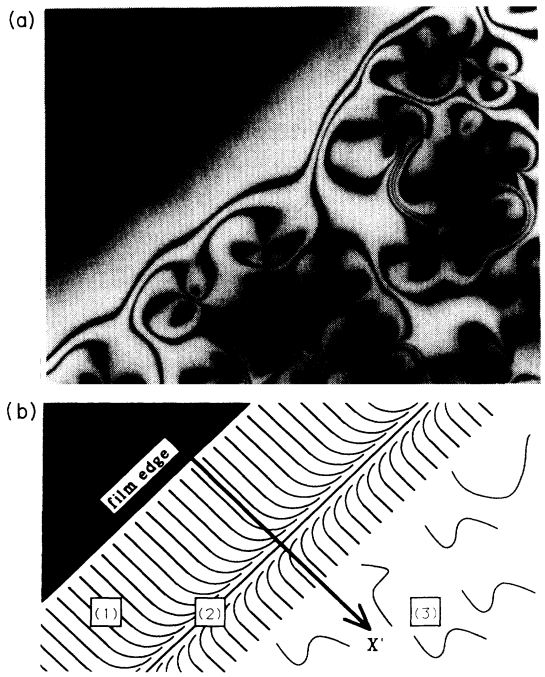

FIG. 3. (a) The polarizing microscope texture of the nematic film with free surface placed onto the glycerine support (×130); (b) the corresponding schema shows the horizontal projection of $\mathbf{n}$.

(2) The intermediate region, where $\mathbf{n}_{xy}$ changes the orientation from $\varphi_0=0$ to $\varphi_0=\pm\pi/2$ thus forming a domain wall. The domain wall is manifested by pair of dark lines. This region is characterized also by the maximal value of the thickness gradient; the latter is manifested by sharp changes in the optical phase difference.

(3) The thick region, which is more close to the film center; here again the azimuthal orientation deviates from $\varphi_0=\pm\pi/2$ and takes different values when one moves towards the center. The textures are nonuniform, but keep some specific order of deformations.

The main feature of the patterns is the unexpected azimuthal rotation of $\mathbf{n}_{xy}$ from $\varphi_0=0$ to $\varphi_0=\pm\pi/2$ and from $\varphi_0=\pm\pi/2$ to $\varphi_0=0$ when one proceeds from the film periphery to the center. However, this behavior becomes clear if one takes into account the geometrical anchoring that is determined by the film profile.

The isotropic part σ of the surface tension at the nematic-isotropic media interface is of the order of 10^{-2} J/m^2 [16] and thus is much greater than the anisotropic one (polar anchoring energy is usually smaller than 10^{-4} J/m^2) and the elastic energy ($\approx 10^{-5}$ J/m^2 for micrometer-thick sample). Hence the nematic film profile should be similar to that expected for the isotropic liquid

films, see, e.g., [14]. For our purposes it is sufficient just to indicate that the nematic film has a thicker central part (3), a thin precursor (1), and an intermediate part (2). The surface tilt γ should vary from $\gamma=0$ at the center to $\gamma\approx 0$ at precursor periphery through some maximal value γ_{max} at intermediate region (2). The observation of interference rings confirms the maximal tilt in the region (2).

The second parameter, $\Delta\bar{\theta}$, also changes along the film. Because of the finite polar anchoring, $\Delta\bar{\theta}$ is thickness dependent; for 1 μm the order of 0.1°–1° is expected. Thus $\gamma/\Delta\bar{\theta}$ varies with film thickness and can be larger or smaller than unity. It leads to different azimuthal orientations of $\mathbf{n}_{xy}$ in different regions of the film. If $\gamma_{max}/\Delta\bar{\theta}>1$, in the region (2) one can observe the orientation of $\mathbf{n}_{xy}$ that is perpendicular to the thickness gradient, $\varphi_{0eq}=\pm\pi/2$, see Eq. (8) and Fig. 2(a). When one moves towards the film precursor (1) or center (3), $\gamma/\Delta\bar{\theta}$ decreases because γ tends to 0. Hence φ_{0eq} must change from $\varphi_{0eq}=\pm\pi/2$ to $\varphi_{0eq}=0$ which is exactly the case of Fig. 3. Since for $\gamma\approx\Delta\bar{\theta}$ the angular dependency of F_A is smooth [Fig. 2(a)], the geometrical anchoring allows the structures in some parts of the regions (1) and (3) to be strongly influenced, for example, by the splay-canceling mechanism [17] or saddle-splay rigidity. It has been already discussed for defects in the thick part (3) [18,19] and for stripe domains in the thin region [15,20].

To conclude, it is shown that the specific azimuthal behavior of the nematic sample occurs when the bounding surfaces are nonparallel. It is expected that the considered geometrical anchoring should be taken into account in many situations with confined liquid-crystalline volumes like cells with oblique evaporated coating, dispersed and sessile drops, and spread films, which are currently receiving great interest.

The author is indebted to G. Barbero, G. Durand, V. Pergamenshchik, and A. Strigazzi for discussions and especially to M. Kléman for support and numerous discussions. The Laboratoire de Physique des Solides is "Unité associeé No. 2 au CNRS."

*Present address: Liquid Crystal Institute, Kent State University, Kent, OH 44242.

[1] P. G. de Gennes, *The Physics of Liquid Crystals* (Clarendon, Oxford, 1974).
[2] M. Kléman, *Points, Lines and Walls in Liquid Crystals, Magnetic Systems and Various Ordered Media* (Wiley, New York, 1983).
[3] J. Cognard, Mol. Cryst. Liq. Cryst. **78**, Suppl. 1, 1 (1982).
[4] L. M. Blinov, E. I. Kats, and A. A. Sonin, Usp. Fiz. Nauk **152**, 449 (1987) [Sov. Phys. Usp. **30**, 604 (1987)].
[5] S. Faetti, Mol. Cryst. Liq. Cryst. **179**, 217 (1990).
[6] R. Williams, Phys. Rev. Lett. **21**, 342 (1968).
[7] R. Williams, J. Chem. Phys. **50**, 1324 (1969).
[8] D. Meyerhofer, A. Sussman, and R. Williams, J. Appl. Phys. **43**, 3685 (1972).
[9] E. F. Carr, Liq. Cryst. **4**, 573 (1989).
[10] G. Srajer, F. Lonberg, and R. B. Meyer, Phys. Rev. Lett. **67**, 1102 (1991).
[11] P. G. de Gennes, Solid State Commun. **8**, 213 (1970).
[12] D. W. Berreman, Phys. Rev. Lett. **28**, 1683 (1972).
[13] G. E. Volovik and O. D. Lavrentovich, Zh. Eksp. Teor. Fiz. **85**, 1997 (1983) [Sov. Phys. JETP **58**, 1159 (1983)].
[14] P. G. de Gennes, Rev. Mod. Phys. **57**, 827 (1985).
[15] O. D. Lavrentovich and V. M. Pergamenschchik, Pis'ma Zh. Tekh. Fiz. **15**, 73 (1989) [Sov. Tech. Phys. Lett. **15**, 194 (1989)]; Mol. Cryst. Liq. Cryst. **179**, 125 (1990).
[16] O. D. Lavrentovich and L. N. Tarakhan, Poverkhnost. Fiz. Khim. Mekh. No. 1, 39 (1990), in Russian.
[17] M. J. Press and A. S. Arrott, J. Phys. (Paris) Colloq. **36**, C1-177 (1975).
[18] O. D. Lavrentovich and Yu. A. Nastishin, Europhys. Lett. **12**, 135 (1990).
[19] O. D. Lavrentovich, Phys. Scr. **T39**, 394 (1991).
[20] A. Sparavigna and A. Strigazzi, Mol. Cryst. Liq. Cryst. (to be published).

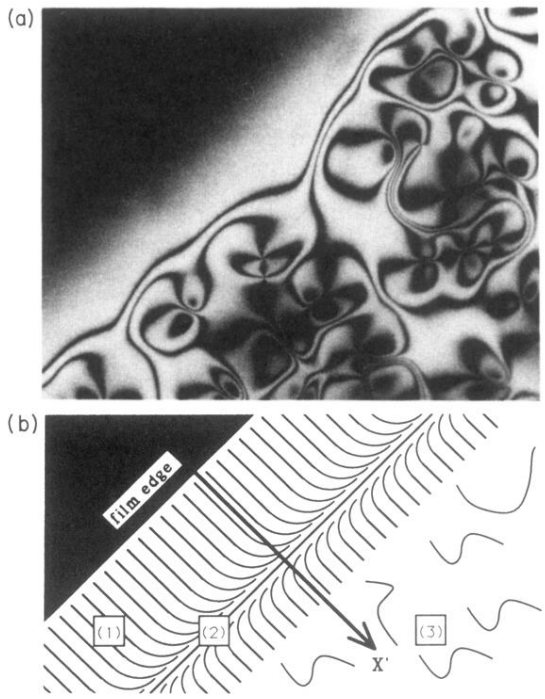

FIG. 3. (a) The polarizing microscope texture of the nematic film with free surface placed onto the glycerine support (×130); (b) the corresponding schema shows the horizontal projection of **n**.